Available online at www.sciencedirect.com

ScienceDirect

ARTICLE

Effect of Volume Fraction on the Coarsening of Pb Nanophase in Al-Pb Nanocomposite Alloys Prepared by High Energy Ball Milling

Wu Zhifang,   Wu Jiang,   Zhang Lei,   Wu Run,   Chang Qingming

The State Key Laboratory of Refractories and Metallurgy, Wuhan University of Science and Technology, Wuhan 430081, China

Abstract: The effect of volume fraction on the coarsening of Pb nanophase in Al-Pb nanocomposite alloys prepared by high energy ball milling has been studied by X-ray diffraction, scanning electron microscopy and transmission electron microscopy. The coarsening of Pb nanophase with different volume fractions in Al-Pb nanocomposite alloys follows the cubic growth law even though the size of the constituent phase is in nanometer range. The coarsening rate of Pb nanophase increases distinctly as the volume fraction increases, and the variation of coarsening rate is greater than the theoretical prediction in this composition range. The activation energy for coarsening of Pb nanophase does not vary with volume fraction. The coarsening of Pb nanophase is controlled by grain boundary diffusion for solute atoms in solvent matrix.

Key words: Pb nanophase coarsening; volume fraction; aluminum alloy; nanocomposite alloys; high energy ball milling

Nanocomposite alloys, which consist of at least two phases in nanometer size, have potential application in the fields of magnetic materials[1], hydrogen storage materials[2], hard metals[3], bearing alloys[4], and so on. The unique nanocomposite structure makes those materials exhibit properties much superior to those with conventional phase size [5,6]. The size, distribution and volume fraction of secondary phase have a very important influence on the properties of nanocomposite alloys [7,8]. Owing to the polydisperse nature of the mixture itself, nanocomposite alloys posses inherently a very high interfacial energy which provides a strong driving force for coarsening of secondary phase. If coarsening of secondary phase occurs, nanocomposite alloys lose their original excellent properties. Thus, to clarify the coarsening of secondary phase in the nanocomposite alloys is of great importance.

For the composite alloys with constant volume fraction ratio and conventional grain size, the self-similar coarsening of dispersed spherical particles embedded in a matrix, also known as Ostwald ripening, is generally described by Lifshitz-Slyozov-Wagner (LSW) theory[9,10]. The LSW theory states that the cube of the average particle radius grows proportional with the annealing time if the mass transport is governed by a diffusion mechanism. Since interparticle diffusional interactions are neglected in LSW theory, this theory is strictly valid only in the physically unrealistic limit of zero volume fraction of secondary phase. As a result, many efforts have been made to modify LSW theory and extend it to nonzero volume fraction of dispersed phases using both analytic and numerical methods[11-15]. All these modern Ostwald ripening theories show that the cubic coarsening law can still be used for embedded phase of high volume fraction and the coarsening rate increases monotonically with volume fraction of secondary phase although the predicted magnitude of the effect varies considerably depending on the theory. This prediction has been confirmed in coarsening of secondary phase of high volume fraction in various kinds of systems[16-18]. However, the effect of volume fraction on the coarsening behavior of secondary phase in composite alloys with conventional

grain size is quite complicated. For example, the coarsening rate of γ' precipitates with small volume fraction in Ni-base alloys decreases as the volume fraction increases[19]. It has also been found that the coarsening rate of Co phase in Cu-Co alloys is not dependent on the volume fraction[20]. Therefore, further investigation is necessary to have thorough understanding on the effect of volume fraction on coarsening of secondary phase in composite alloys.

For the nanocomposite alloys, research has been focused mainly on the coarsening of secondary phase. For example, the coarsening of secondary phase in Ni-TaC nanocomposite alloy follows the quadruplicate growth law and is controlled by grain-boundary diffusion [21]. For another instance, the coarsening of secondary phase in Cu-Ag nanocomposite alloys follows the cubic growth law and the activation energy for coarsening of secondary phase is different from that of conventional grain sized alloys[22]. It is therefore of significance to investigate the coarsening of secondary phase in the nanocomposite alloys in more details. On the other hand, we know relatively little is known about the effect of volume fraction on coarsening of secondary phase in the nanocomposite alloys; in particular, it is not clear whether predictions of modern Ostwald ripening theories are still valid when the size of both matrix phase and secondary phase is in nanometer range.

In the present work, the effect of volume fraction on coarsening of Pb nanophase in Al-Pb nanocomposite alloys prepared by high energy ball milling has been studied. This is because Al-Pb is a typical immiscible system and the Al-Pb nanocomposite alloys fabricated by high energy ball milling exhibit super wear resistance which is very much dependent on the grain size (and/or phase size) and volume fraction of Pb phase[4]. Therefore, a study of the effect of volume fraction on coarsening of Pb nanophase in Al-Pb nanocomposite alloys is significant to both the fundamental research of nanocomposite alloys and their application in engineering.

1 Experiment

Al and Pb powders of 99.9% purity with the average particle size of 70~80 μm were used as raw materials. Alloys with composition of Al-2.5wt%Pb, Al-5wt%Pb and Al-10wt%Pb were selected, in which the volume fraction of Pb phase is 0.33%, 0.68% and 1.42%, respectively, and Pb phase is hence regarded as secondary phase with different volume fractions. The powder mixtures of selected composition were sealed in stainless steel vials together with hardened steel balls. The mass ratio of the powders to balls was 1 to 10. The handling of powders were performed inside a glove filled with pure argon. The milling process was performed in a QM-3SP4 planetary ball mill. The milled powders were uniaxially cold pressed under a pressure of 440 MPa to get bulk samples. The as-compacted bulk samples

were then heated at different temperatures for different time under the protection of pure argon atmosphere. A Philips X'Pert MPD X-ray diffractometer (XRD) using Cu Kα radiation (λ=0.1541nm), a FEI-Navo Nano scanning electron microscope (SEM) and a JEM-2100 transmission electron microscope (TEM) were used to characterize the microstructure.

2 Results and Discussion

Fig.1 shows the X-ray diffraction patterns of Al-Pb alloys with different volume fractions of Pb phase after ball milling for 30 h. It is clearly seen that only diffraction peaks of both Al and Pb phases are observed; shifts of peak positions have not been detected. No trace of amorphous or other intermediate phases is found. It is also evident that the diffraction peaks of Al and Pb phases are broadened after milling for 30 h, and the peaks of Pb are broadened more obviously than those of Al in Al-Pb alloys. These results are attributed to the remarkable grain refinement of Al and Pb phases in as-milled Al-Pb alloys, and the refining of the Pb phase is much more obvious. As estimated from the diffraction peak broadening by the Vogit method [23], the average grain sizes of Al and Pb phases in as-milled Al-Pb alloys are approximately 80 and 10 nm, respectively. It means that the Al-Pb nanocomposite alloys with different volume fractions of Pb nanophase have been prepared by high energy ball milling.

Fig.2 shows the back scattering electron (BSE) images, in which the dark and bright region represent the Al matrix and Pb particle, respectively, of Al-Pb samples after 30 h of milling. The SEM observation shows that Pb particles with nanometer sizes are distributed in the Al matrix. TEM observations provide more details of the microstructures of as-milled products. Fig.3 shows nanosized Pb phase particles obtained in the Al-Pb samples milled for 30 h, and they are similar to those reported[24], which proves that all Pb phase are single crystal particles and uniformly distributed in the Al matrix. Therefore, the grain size of Pb phase estimated from XRD analysis actually corresponds to
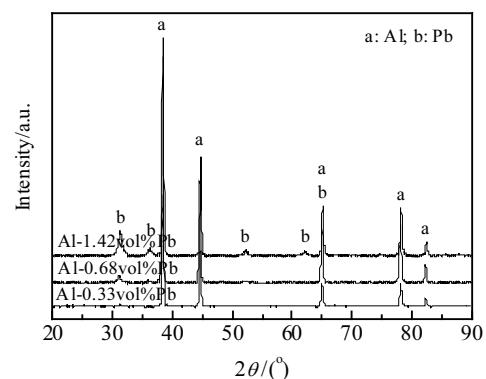

Fig.1 XRD patterns of Al-Pb alloys with different volume fractions of Pb phase after ball milling for 30 h
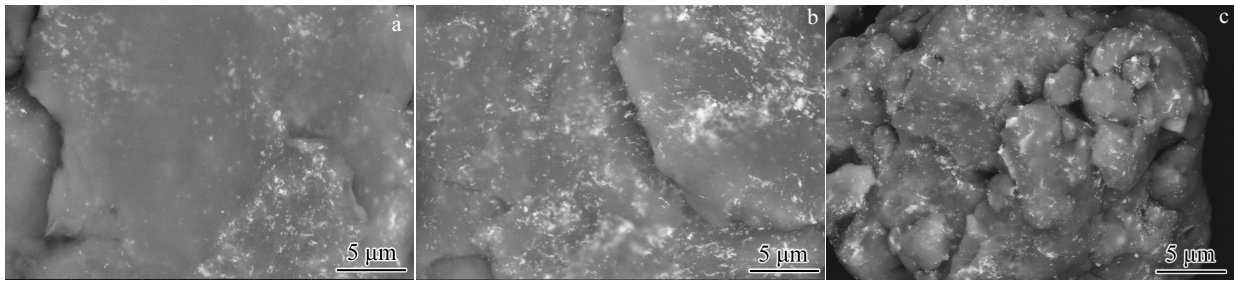
Fig.2　SEM micrographs of Al-Pb alloys with different volume fractions of Pb nanophase after ball milling for 30 h: (a) Al-0.33vol%Pb, (b) Al-0.68vol%Pb, and (c) Al-1.42vol%Pb
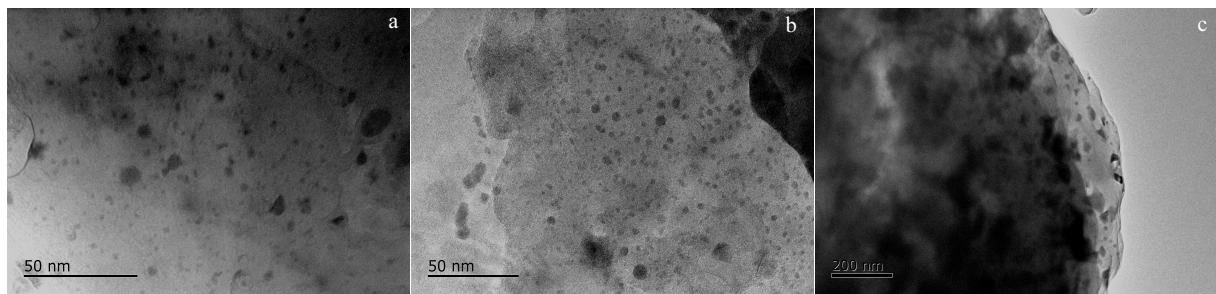

Fig.3　TEM bright field images of Al-Pb alloys with different volume fractions of Pb nanophase after ball milling for 30 h: (a) Al-0.33vol%Pb, (b) Al-0.68vol%Pb, and (c) Al-1.42vol%Pb

the particle size of Pb phase in Al-Pb nanocomposite alloys with different volume fractions of Pb nanophase. The average grain sizes of Pb phase with different volume fractions are about 10 nm, which are in good agreement with the XRD results.

Fig.4 shows X-ray diffraction patterns of the as-milled Al-Pb alloys with different volume fractions of Pb nanophase heated at 673 K for 1 h. It can be observed that there are only diffraction peaks of Al and Pb phase. It is obvious that diffraction peaks sharpen with increase of volume fractions of Pb nanophase which indicates the coarsening of Al and Pb phase after heating.

Fig.5 shows the BSE images of Al-Pb alloys with different volume fractions of Pb nanophase heated at 673 K for 1 h after 30 h of milling. The SEM observation shows that the Pb nanophase grows upon heating and has homogeneous size distribution. It also indicates that the size of Pb nanophase slightly increases as the volume fraction increases in Al-Pb nanocomposite alloys under the same heating condition. This is in agreement with the XRD analysis described in a previous section.

Fig.6 shows the dependence of Pb nanophase size on heating dwelling time in as-milled Al-Pb alloys with different volume fractions of Pb nanophase at heating temperature 673 K. It is clear that there exists an excellent linear correlation between the cubic Pb nanophase size (r)
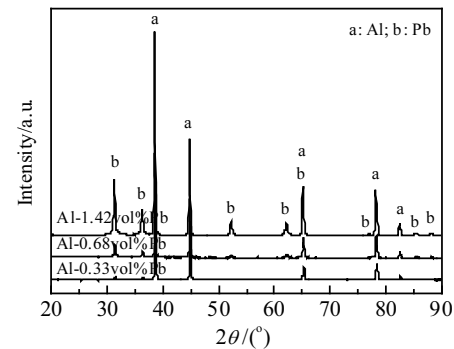

Fig.4　X-ray diffraction patterns of the as-milled Al-Pb alloys with different volume fractions of Pb nanophase heated at 673 K for 1 h

and the dwelling time (t) for Al-Pb nanocomposite alloys with different volume fractions of Pb nanophase at the used heating temperature. Here, r_0 is the average radius of the phase in the as-milled condition; this is measured as 5 nm. It should be noted that the above linear relationship (Fig.6) also exists for the Al-Pb alloys with different volume fractions of Pb nanophase heated at 573, 623 and 723 K. Moreover, it is worth indicating that other power-law dependences, such as r^4 and r^6, do not yield a satisfactory fitting to the experimental data. The excellent linear
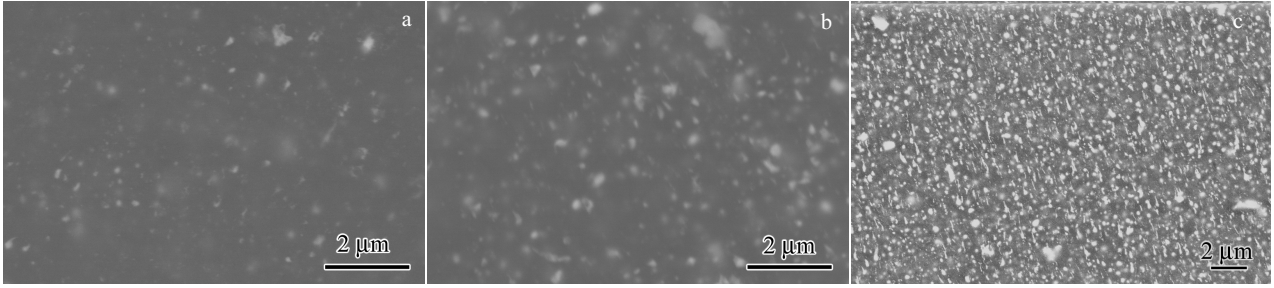
Fig.5   SEM micrographs of Al-Pb alloys with different volume fractions of Pb nanophase heated at 673 K for 1 h from the Al-Pb alloy powders milled for 30 h: (a) Al-0.33vol%Pb, (b) Al-0.68vol%Pb, and (c) Al-1.42vol%Pb
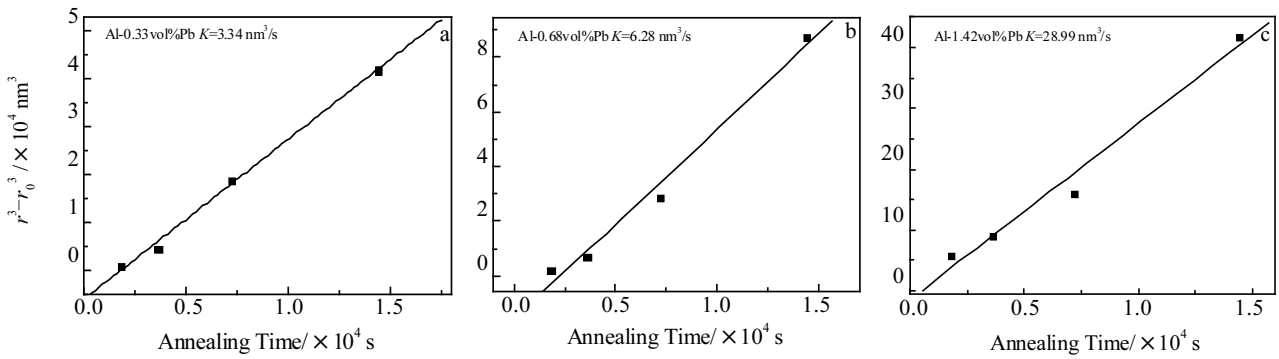

Fig.6   Dependence of the size of Pb phase on heating time in as-milled Al-Pb alloys with different volume fractions of Pb nanophase at heating temperature of 673 K: (a) Al-0.33vol%Pb, (b) Al-0.68vol%Pb, and (c) Al-1.42vol%Pb

relationship between the cubic r and time (t) is just what the diffusion controlled Ostwald ripening theory describes.

In the modern Ostwald ripening theories accounting for the effect of volume fraction of secondary phase, the time dependency of the size of a coarsening particle or phase is formulated by the equation as follows[25,26]:

$$r^3 - r_0^3 = K(\phi) \cdot t \tag{1}$$

where ϕ is the volume fraction of secondary phase, $K(\phi)$ is the coarsening rate, which can be obtained from the slope of the straight lines correlated between the cubic r and time (t), like those in Fig.6. The expression for $K(\phi)$ is given by

$$K(\phi) = \frac{A(\phi) C_e \Omega^2 \gamma D}{RT} \tag{2}$$

Here, $A(\phi)$ is a dimensionless constant and $A(0)=8/9$; thus, the theories are simplified to the LSW theory in the limit of zero volume fraction. The magnitude of the dimensionless constant $A(\phi)$ depends on the volume fraction of secondary phase and is a monotonically increasing function of the volume fraction of secondary phase. C_e is the equilibrium solute content of the matrix, Ω is the molar volume of the precipitate, γ is the surface energy per unit area of the matrix-particle phase boundary, D is the diffusion coefficient of the constitutive particle element in the matrix, R is the universal gas constant, 8.31 J·(mol/K)$^{-1}$ and T is the coarsening temperature.

The diffusion coefficient D can be expressed in an Arrhenius type equation:

$$D = D_0 \exp(-\frac{Q}{RT}) \tag{3}$$

where D_0 is pre-exponential factor and Q is the activation energy for coarsening of secondary phase. The activation energy Q is often used to characterize the mechanism dominating coarsening.

In Fig.6, it is apparent that the value of coarsening rate of Pb nanophase increases significantly as the volume fraction increases under the same heating condition. In other words, the volume fraction of Pb nanophase in Al-Pb nanocomposite alloys has an obvious effect on the coarsening of Pb nanophase. Table 1 shows that $K(\phi)$ increases with increasing Pb nanophase volume fraction. This result is the most direct evidence that the coarsening in this system is controlled by diffusion. The observed increase of $K(\phi)$ with ϕ is more rapid than that predicted by Ardell[11], Brailsford and Wynblatt[12] in this composition range.

If Eq.(2) is rearranged as:

$$\frac{K(\phi)T}{C_e} = \frac{A(\phi) \Omega^2 \gamma D}{R} \tag{4}$$

The right hand side of Eq.(4) can reasonably be taken as dependent only on temperature through D, suggesting that

Table 1   Experimental value for $K(\phi)$ of the specimens annealed at 673 K and their ratio to the value of Al-0.33vol%Pb compared to the theoretical results of Adrell[11], Brailsford and Wynblatt[12]

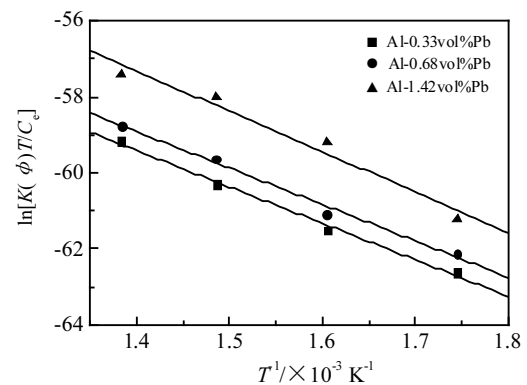| Composition	Experimental $K(\phi)$/ $\times 10^{-27}$ m³·s⁻¹	Observed $K(\phi)/K(0.0033)$	Theoretical $K(\phi)/K(0.0033)^{[11]}$	Theoretical $K(\phi)/K(0.0033)^{[12]}$
Al-0.33vol%Pb	3.34	1	1	1
Al-0.68vol%Pb	6.28	1.88	1.18	1.08
Al-1.42vol%Pb	28.99	8.68	1.47	1.16

$\ln[K(\phi)T/C_e]$ be plotted against $(1/T)$. Eq. (4) can be rearranged to give:

$$\ln[\frac{K(\phi)T}{C_e}] = \text{Cons} \tan t - \frac{Q}{RT} \qquad (5)$$

Thus plots of $\ln[K(\phi)T/C_e]$ versus $(1/T)$ yield Q from the slope. In order to estimate the Q in Al-Pb nanocomposite alloys with different volume fractions of Pb nanophase, we got the solubility of Pb in Al solid-solution at different temperatures (573, 623, 673 and 723 K) according to Ref.[27]. The activation energies for coarsening of Pb nanophase in Al-Pb nanocomposite alloys can be subsequently obtained from the slope of plots of $\ln[K(\phi)T/C_e]$ against $1/T$ as shown in Fig.7. The overall data in Fig.7 fit excellently to straight lines. Thus, the activation energies for coarsening of Pb nanophase of different volume fractions were obtained, as given in Table 2. The activation energies for coarsening of Pb nanophase of different volume fractions in Al-Pb nanocomposite alloys do not show any systematic change with alloy composition and this result is similar to those of composite alloys with conventional grain size[29]. The average value of activation energy for coarsening of Pb nanophase obtained in this work is 82.48 kJ/mol for the Al-Pb nanocomposite alloys. For comparison, the diffusion activation energy of Pb in Al of different diffusion mechanisms is given in Table 2. It shows that the value obtained in this work is much smaller than that of lattice diffusion mechanism of Pb in Al and lattice self-diffusion of Al but very close to that of boundary self-diffusion of Al. This indicates that the coarsening mechanism of secondary phase in the nanocomposite alloys is different from that in conventional

composite alloys. The observation of the cubic law for coarsening of secondary phase in the nanocomposite alloys reveals that the coarsening process is controlled by the three-dimensional long distance diffusion of solute atoms. However, the agreement of the activation energy to that of grain boundary self-diffusion of matrix indicates that the diffusion mechanism in the nanocomposite alloys is basically grain boundary diffusion. This is because the grain sizes of matrix phase and secondary phase are all in nanometer range. Thus, the solute atoms should diffuse more easily along nanocrystalline boundary than in conventional dual-phase systems.

As mentioned before, the observed increase of $K(\phi)$ with the volume fraction of Pb nanophase in Al-Pb nanocomposite alloys is more rapid than that predicted by the modern Ostwald ripening theories in this composition range. This may be related to the coarsening mechanism of Pb nanophase. The coarsening of Pb nanophase in Al-Pb

Fig.7   Determination of the activation energy (Q) for coarsening of Pb nanophase in Al-Pb nanocomposite alloys

Table 2   Activation energy of experiment and theory in Al-Pb system (kJ/mol)

Composition	Activation energy of our result	Activation energy of lattice diffusion[28]	Activation energy of lattice (self-) diffusion[28]	Activation energy of grain boundary (self-) diffusion[28]
Al-0.33vol%Pb	88.27	Pb in Al: 145.6 (777~876 K)	Pb: 107.4 (473~596 K) Al: 142.4 (723~923 K)	Pb: 66 (487~533 K) Al: 90 (623~753 K)
Al-0.68vol%Pb	79.64		144.4 (573~923 K)	
Al-1.42vol%Pb	79.54		123.5 (298~581 K) 126.4 (358~482 K)	

nanocomposite alloys is controlled by the grain boundary diffusion. While in modern Ostwald ripening theories, the coarsening of secondary phase is controlled by the lattice diffusion. At the same volume fraction of secondary phase, the solute atoms diffuse more easily along nanocrystalline boundary than that of lattice. This results in the rapid increase of $K(\phi)$ with the volume fraction of Pb nanophase in Al-Pb nanocomposite alloys.

3 Conclusions

1) The coarsening of Pb nanophase with different volume fractions in Al-Pb nanocomposite alloys follows the cubic growth law even though the size of the constituent phase is in nanometer range.

2) The coarsening rate of Pb nanophase increases distinctly as the volume fraction increases, and the variation of coarsening rate is greater than the theoretical prediction in this composition range.

3) The activation energy for coarsening of Pb nanophase does not vary with alloy composition. The coarsening of Pb nanophase is controlled by grain boundary diffusion for solute atoms in solvent matrix.

References

1　Betancourt J I, Davies H A. *Journal of Magnetism and Magnetic Materials*[J], 2002, 246(1-2): 6

2　Zhu M, Wang H, Ouyang L Z *et al. International Journal of Hydrogen Energy*[J], 2006, 31(2): 251

3　Cha S I, Hong S H, Ha G B *et al. Scripta Mater*[J], 2001, 44(8-9): 1535

4　Zhu M, Gao Y, Chuang C Y *et al. Wear*[J], 2000, 242(1-2): 47

5　Sharma A S, Biswas K, Basu B. *Metallurgical and Materials Transactions A*[J], 2014, 45(1): 482

6　Liu X, Zeng M Q, Ma Y *et al. Wear*[J], 2012, 294(31): 387

7　Liu X, Zeng M Q, Ma Y *et al. Materials Science and Engineering A*[J], 2009, 506(1-2): 1

8　Sheng H W, Zhou F, Hu Z Q *et al. Journal of Materials Research*[J], 1998, 13(2): 308

9　Lifshitz I M, Slyozov V V. *Journal of Physics and Chemistry of Solids*[J], 1961, 19(1-2): 35

10　Wagner C. *Berichte Der Bunsengesellschaft Für Physikalische Chemie*[J], 1961, 65: 581

11　Ardell A J. *Acta Metallurgica*[J], 1972, 20(1): 61

12　Brailsford A D, Wynblatt P. *Acta Metallurgica*[J], 1979, 27(3): 489

13　Davies C K L, Nash P, Stevens R N. *Acta Materialia*[J], 1980, 28(2): 179

14　Tokuyama M, Kawasaki K. *Physica A*[J], 1984, 123(2-3): 386

15　Voorhees P W, Glicksman M E. *Metallurgical Transactions A*[J], 1984, 15(6): 1081

16　Ma Y, Ardell A J. *Acta Materialia*[J], 2007, 55(13): 4419

17　He Y B, Ye S Y, Naser J *et al. Journal of Materials Science*[J], 2000, 35(23): 5973

18　Rowenhorst D J, Kuang J P, Thornton K *et al. Acta Materialia*[J], 2006, 54(8): 2027

19　Ardell A J. *Scripta Metallurgica et Materialia*[J], 1990, 24(2): 343

20　Bender W, Ratke L. *Scripta Metallurgica et Materialia*[J], 1993, 28(6): 737

21　Wilde J R, Greer A L. *Materials Science and Engineering A*[J], 2001, 304-306: 932

22　Zhu M, Wu Z F, Zeng M Q *et al. Journal of Materials Science*[J], 2008, 43(9): 3259

23　Langford J L. *Journal of Applied Crystalline*[J], 1978, 11(1): 10

24　Gabrisch H, Kjeldgaard L, Johnson E *et al. Acta Materialia*[J], 2001, 49(20): 4259

25　Baldan A. *Journal of Materials Science*[J], 2002, 37(11): 2171

26　Baldan A. *Journal of Materials Science*[J], 2002, 37(12): 2379

27　Ma E, He J H, Schilling P J. *Physical Review B: Condensed Matter*[J], 1997, 55(9): 5542

28　Gale W E, Totemeier T C. *Smithells Materials Reference Book*[M]. Butterworth-Heinemann, 2004: 11

29　Kang S S, Yoon D N. *Metallurgical Transactions A*[J], 1982, 13(8): 1405

高能球磨制备 Al-Pb 纳米相复合结构合金中纳米相 Pb 体积分数对其长大行为影响

吴志方，吴 江，张 磊，吴 润，常庆明
(武汉科技大学 省部共建耐火材料与冶金国家重点实验室，湖北 武汉 430081)

摘 要：利用 X 射线衍射仪、扫描电子显微镜和透射电子显微镜研究了高能球磨制备的 Al-Pb 纳米相复合结构合金中纳米相 Pb 的体积分数对其长大行为的影响。结果表明，尽管 Al-Pb 纳米相复合结构中组成相的尺寸均在纳米量级，不同体积分数的纳米相 Pb 的长大行为均遵循三次方定律。纳米相 Pb 的粗化速率随其体积分数的增加而增加，增加幅度大于理论在此成分范围内的预测。纳米相 Pb 的粗化激活能不随合金成分而变化。纳米相 Pb 的粗化受溶质原子沿溶剂基体的晶界扩散所控制。

关键词：纳米相粗化体积分数；铝合金；复合结构合金；高能球磨

作者简介：吴志方，女，1977 年生，博士，副教授，武汉科技大学省部共建耐火材料与冶金国家重点实验室，湖北 武汉 430081，E-mail: wuzhifang@wust.edu.cn